We are IntechOpen,
the world's leading publisher of
Open Access books
Built by scientists, for scientists

4,800

Open access books available

122,000

International authors and editors

135M

Downloads

154

Countries delivered to

Our authors are among the

TOP 1%

most cited scientists

12.2%

Contributors from top 500 universities

CLARIVATE ANALYTICS

BOOK CITATION INDEX

INDEXED

WEB OF SCIENCE™

Selection of our books indexed in the Book Citation Index
in Web of Science™ Core Collection (BKCI)

Interested in publishing with us?
Contact book.department@intechopen.com

Numbers displayed above are based on latest data collected.
For more information visit www.intechopen.com

Large Arrays and Networks of Carbon Nanotubes: Morphology Control by Process Parameters

I. Levchenko, Z.-J. Han, S. Kumar, S. Yick, J. Fang and K. Ostrikov

Additional information is available at the end of the chapter

1. Introduction

Large arrays and networks of carbon nanotubes, both single- and multi-walled, feature many superior properties which offer excellent opportunities for various modern applications ranging from nanoelectronics, supercapacitors, photovoltaic cells, energy storage and conversation devices, to gas- and biosensors, nanomechanical and biomedical devices etc. At present, arrays and networks of carbon nanotubes are mainly fabricated from the pre-fabricated separated nanotubes by solution-based techniques. However, the intrinsic structure of the nanotubes (mainly, the level of the structural defects) which are required for the best performance in the nanotube-based applications, are often damaged during the array/network fabrication by surfactants, chemicals, and sonication involved in the process. As a result, the performance of the functional devices may be significantly degraded. In contrast, directly synthesized nanotube arrays/networks can preclude the adverse effects of the solution-based process and largely preserve the excellent properties of the pristine nanotubes. Owing to its advantages of scale-up production and precise positioning of the grown nanotubes, catalytic and catalyst-free chemical vapor depositions (CVD), as well as plasma-enhanced chemical vapor deposition (PECVD) are the methods most promising for the direct synthesis of the nanotubes.

On the other hand, these methods demonstrate poor controllability, which results in the unpredictable properties, structure and morphology of the resultant arrays. In our paper we will discuss our recent results obtained by the application of CVD and PECVD methods. Specifically, we will discuss carbon nanotube arrays and networks of very different morphology. The fabrication of the arrays of vertically aligned and entangled nanotubes, as well as arrays of arbitrary shapes grown directly on the pre-patterned substrates will be considered with a special attention paid to the fabrication methods and the influence of the process parameters on the array

growth morphology (see Figure 1). Besides, the possibility of creating the 3D structures of carbon nanotubes through post-processing of the arrays by liquids will be discussed.

The fabrication methods involved are the conventional CVD utilizing various gases such as methane, ethane, acetylene, argon, and hydrogen; plasma-enhanced CVD based on inductively-coupled low-temperature plasma reactor; microwave PECVD. The advantages of the plasma-based CVD process will be shown and discussed with a special attention. We will also discuss the influence of the process parameters such as process temperature, pressure, gas composition, discharge power etc. on the morphology of the nanotube arrays and networks, and demonstrate that the proper selection of the parameters ensures very high level of the process controllability and as a result, sophisticated control and tailoring of the growth structure and morphology of the carbon nanotube arrays.

Characterization technologies used are scanning and transmission electron microscopy (SEM and TEM), as well as atomic force microscopy (AFM), Raman and X-ray photoelectron spectroscopy techniques. The results of the numerical simulations will also be used to support the growth models and proposed growth mechanisms.
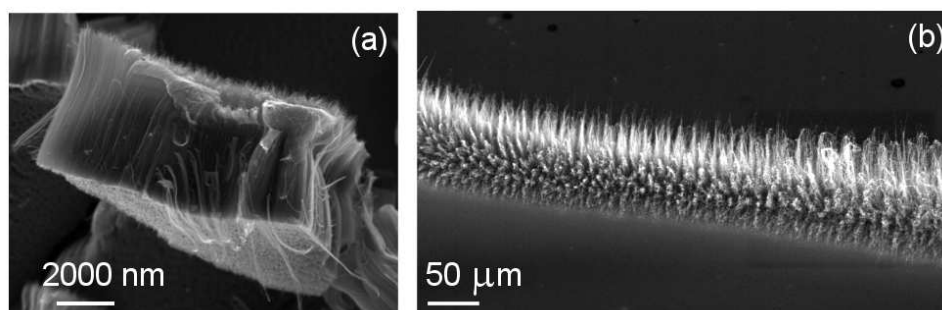

Figure 1. Morphologies of the representative CNT arrays grown by CVD (a) and PECVD (b).

2. CVD versus PECVD: Morphology control issues

2.1. CVD and PECVD: General

The term 'chemical vapor deposition', or 'CVD', is commonly used for describing the processes and chemical reactions which occur in a solid material deposited onto a heated substrate using a gaseous precursor. However, more complicated process than the 'common' CVD takes place [1,2] during the growth of CNTs. In this case, the carbon-containing gaseous precursors (e.g., CH_4, C_2H_4, C_2H_2, CO) firstly dissociate into atomic or molecular carbon species on the surface of catalyst nanoparticles, and then the nucleation occurs as these carbon species diffuse into the catalyst nanoparticles, reach a supersaturated state, and then segregate from the surface of nanoparticles to form a nanotube cap. Subsequently, the growth of nanotubes is sustained by the continuous incorporation of carbon atoms *via* bulk and/or surface diffusion. Figure 2 shows the SEM image of randomly-oriented SWCNTs with a unique 'bridging' morphology in catalytic

CVD. This array was grown by using $Ar/H_2/CH_4$ gas mixture on Fe/Al_2O_3 catalyst. By tuning the growth condition (e.g., temperature and pressure), it was demonstrated that the SWCNTs could be of a high quality (a high I_G/I_D in the Raman spectra) and could contain a significantly higher content of metallic nanotubes as compared to the 'standard' metallic nanotube content of 33% (1/3 metallic and 2/3 semiconducting) produced in many CVD processes [3].

On the other hand, PECVD refers to the CVD process that uses plasma environment as an extra dimension to control the growth of CNTs. Plasma by definition contains ionized species and is generally considered as the fourth state of matter along with solid, liquid and gas. Recent advances in the plasma-based nanofabrication offer unprecedented control over the structure and surface functionalities of a range of nanomaterials [4]. One of the major advantages, as compared to the conventional CVD processes, is that nanostructures can grow vertically-aligned due to the electrical field in the vicinity of surface [5]. Another benefit of using plasma is that the temperature required to dissociate carbon feedstock could be greatly reduced [6]. Figure 3 illustrates the isolated CNTs grown in a PECVD system using Ni/SiO_2 as the catalyst, C_2H_2/NH_3 as the gas precursors, and a DC glow discharge. It can be seen clearly that these nanotubes are aligned vertically to the substrate surface, due to the plasma sheath-directed growth. These freestanding nanotubes could give many opportunities to custom-design novel functional devices.
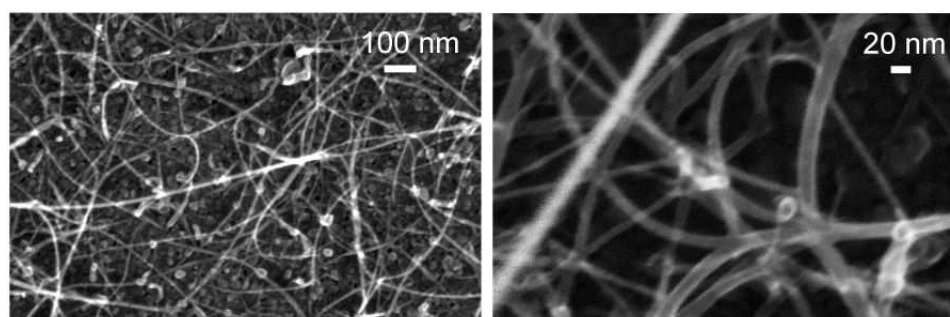

Figure 2. Typical randomly-oriented SWCNT networks with a unique "bridging" morphology grown in catalytic CVD [3].
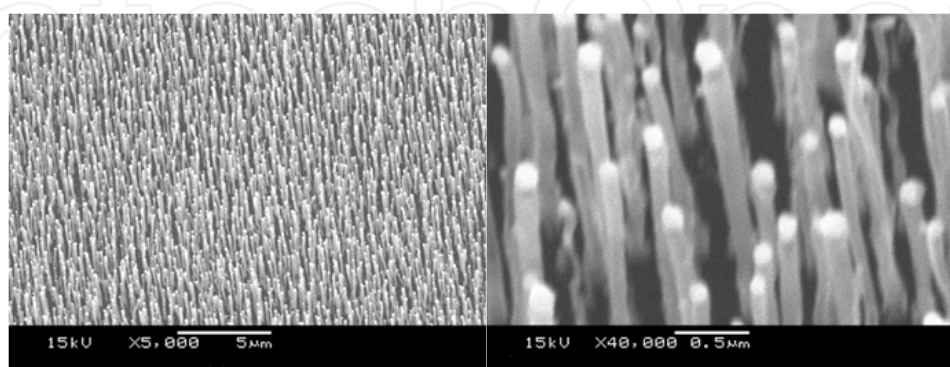

Figure 3. Low- and high-resolution SEM images of the typical arrays of vertically-aligned CNTs grown in PECVD process with a glow discharge. The growth followed the 'tip-growth' mode as the catalyst nanoparticles are noticeable on the top of each nanotube [4].

2.2. Morphologies of nanotube arrays

In general, there are three types of morphologies observed in the directly-grown nanotube arrays: entangled, horizontally aligned, and vertically aligned. Each of these morphologies has their specific functionalities and can be desirable for different applications. In this work, we will briefly describe the first two morphologies and then pay the most attention to the arrays of vertically aligned nanotubes.

The horizontally-aligned CNT arrays were usually grown on the quartz wafers using CVD. The alignment could in such arrays be controlled by two factors: gas flow direction and substrate lattice. These arrays could have a very high density (up to 50 SWNT/μm) over large area. These nanotubes have also a large diameter and good electrical properties desirable for the nanoelectronic applications [7].

On the other hand, the vertically aligned CNTs could be grown using both CVD and PECVD. *Hata et al.* demonstrated that by using Fe/Al_2O_3 as the catalysts, C_2H_4 as the feedstock and a trace amount of water vapor (100 – 300 ppm) as the growth enhancer, high-yield, milli-meter long vertically aligned SWCNTs could be produced [8]. Water in this process was used to etch the possible amorphous carbon phase deposited onto the catalyst during the growth, therefore enhancing the lifetime and activity of the catalyst. The vertical alignment was supported by the collective van der Waals' interactions among the nanotubes [9]. In contrast, the CNTs grown in PECVD process do not require such growth enhancer to align them vertically, since the electrical field in the plasma-surface sheath at the vicinity of the substrate could easily direct the growth.

The third type of CNT arrays is the entangled network consisting of interconnected randomly-oriented nanotubes. In some cases, these networks are not entirely 'random'; instead, they may form certain unique features such as the 'Y-junctions', as well as 'knotted' and 'bridging' structures. *Sun et al.* demonstrated that by using a porous membrane filter to collect the nanotubes at room temperature, a unique 'Y-junction' with high electronic performance could be induced in an aerosol CVD process [10]. Similar to VACNTs, they can be produced in both CVD and PECVD processes. Figure 4 illustrates both the horizontally and vertically aligned morphologies obtained by our group.
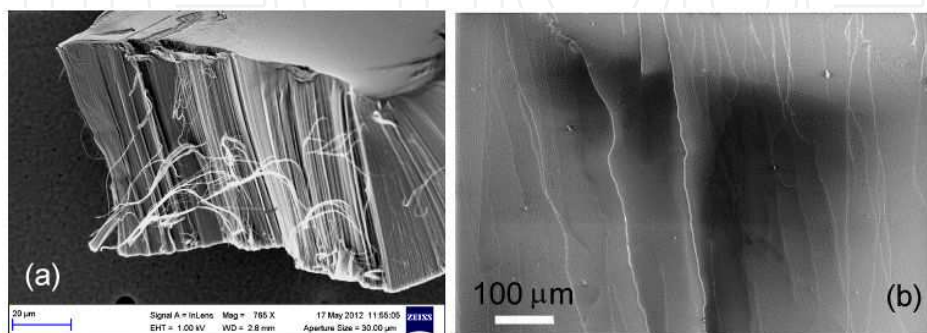

Figure 4. Highly uniform, dense array of vertically aligned single-walled carbon nanotubes (SWCNTs) grown on trilayered $Fe/Al_2O_3/SiO_2$ catalyst (a). Horizontally-aligned nanotubes (b).

2.3. Vertically-aligned arrays of carbon nanotubes

Vertically-aligned CNTs not only preserve the excellent intrinsic properties of individual nanotubes, but also show a high surface-to-mass ratio owing to their three-dimensional microstructure. Moreover, the surface of the vertically-aligned CNTs could be easily function-alized. These advantageous features have placed the vertically-aligned CNT arrays among the most promising materials for a variety of applications ranging from field emitters, heat sinks, nanoelectrochemical systems, gas- and bio-sensors, drug delivery systems, to molecular/particular membranes. For example, Wu et al. used the functionalized vertically-aligned CNTs to deliver nicotine for therapeutic purposes [11]; Han et al. studied the release behaviors of bone morphogenetic protein-2 (BMP-2; a growth factor for human mesenchymal stem cells) on the vertically-aligned CNTs with different surface wettability, in attempting to control the differentiation and proliferation of these stem cells [12].

Growth of the vertically-aligned CNTs can be easily obtained in PECVD. Figure 5 shows SEM images (high and low magnification) of the vertically-aligned nanotubes grown in the low-temperature plasma [13]. These CNTs have a diameter of 50-200 nm, a height of several micrometers, and followed a "tip-growth" mechanism. Interesting, they collapse upon liquid wetting (this will be discussed in more detail in the next section).
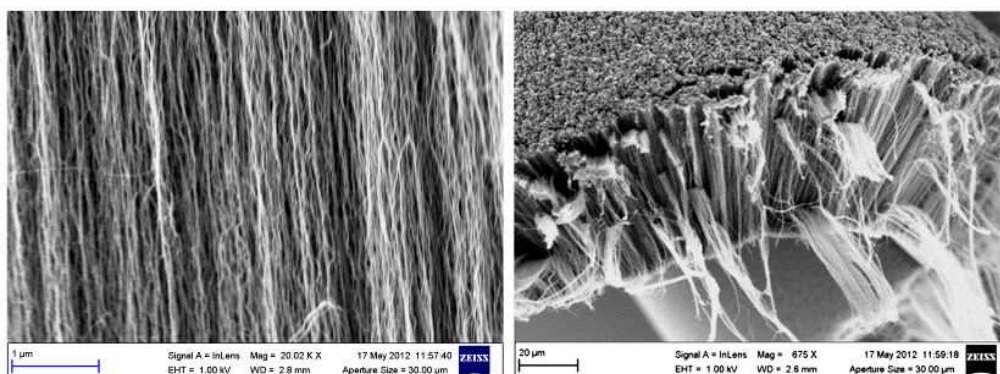

Figure 5. Dense array of vertically aligned single-walled carbon nanotubes.

The the vertically-aligned CNTs grown using CVD process are much denser and longer, and have more uniform distribution of diameters. In such arrays, very strong Van der Waals forces are present. The CVD process is therefore suitable for mass production of CNTs, and may contribute to lowering the price of CNTs. We have recently demonstrated that highly uniform and dense arrays of SWCNTs with more than 90% population of thick nanotubes (>3 nm in diameter) could be obtained by tailoring the thickness and microstructure of the catalyst supporting SiO_2 layer [14].

2.4. Entangled arrays of carbon nanotubes

Networks of entangled nanotubes consist of randomly-oriented nanostructures. The thickness of the entangled array may vary from sum-monolayer to a few monolayers. Advantages of

such morphology, as compared to individual nanotubes, are scalability, stability, reproducibility, and low cost of the CNT-based devices. They are therefore widely used as thin film transistors, transparent conductive coatings, solar cells, gas and biosensors. The electrical resistivity in entangled SWCNTs is determined by the nanotube-nanotube junctions in the network, and the nanotube-metal junctions at the electrodes (so-called Schottky barrier). The intrinsic resistance of the nanotubes usually plays a minor role if the array density is not far away from the percolation threshold [15]. In addition, it is generally perceived that for the CNT-based device to deliver outstanding performance, chirality-selected growth of CNT is a pre-requisite. However, for entangled SWCNTs, this stringent requirement may be avoided if the density is within a certain range (usually 1–3 nanotubes/μm^2) [16,17,18].

There are many parameters of the CVD process that should be controlled to grow entangled CNTs with some special patterns. For example, the length of the nanotubes could be determined by the exposure time of the carbon feedstocks. Recently, we have demonstrated that the density of entangled SWCNTs, which is a critical factor in device performance, could be controlled over 3-order-of-magnitude in acetylene-modulated CVD processes (Figure 6a) [2]. In addition, we also obtained a special 'knotted' morphology of the CNT network by using porous silica as the catalyst-supporting layer (Figure 6b) [19]. In contrast to this morphology, a much lower density of nanotubes was observed on flat silica surface.
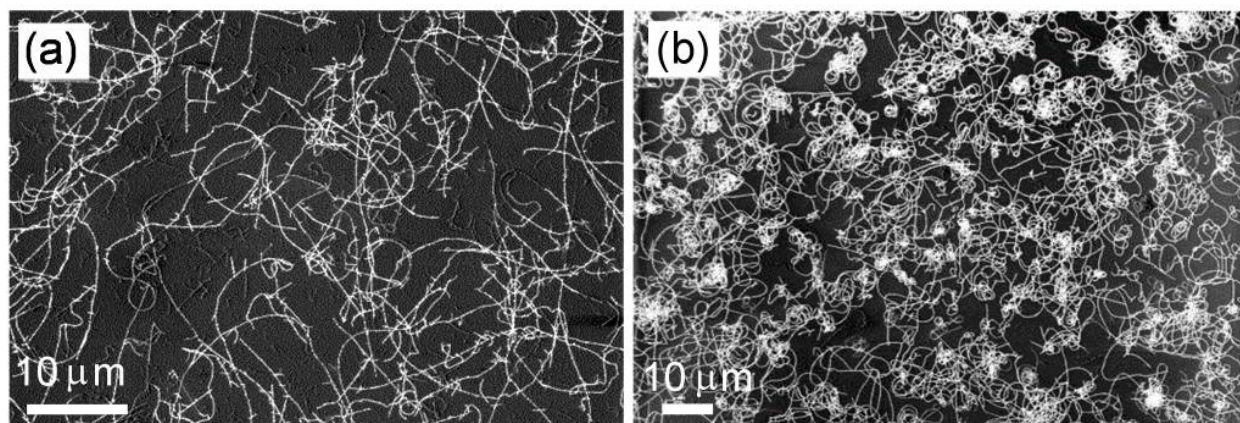

Figure 6. Representative arrays of entangled carbon nanotubes [2,19].

3. Complex catalyst-free arrays by mechanical writing

Plasma-based techniques yet being capable of producing high-quality nanotube arrays, still require metal catalyst to initialize the control the nanotube growth process. However, there is a strong demand in metal-free CNTs, i.e. the CNTs not containing a catalyst metal which is usually incorporated in the nanotube structure (from the nanotube top or bottom, depending on the process used). Removal of metal catalyst from CNTs implies a complex post-processing [20] which results in significant disadvantages, such as essential change in electronic properties

or degradation of the nanotube ordering or orientation (in particular, post-processing deteriorates the vertical orientation of the nanotubes), damages the substrate structure in high temperature annealing process, etc. Thus, removal of the metallic catalyst by after-growth post-processing is feasible only for limited small-scale experimental production [21]. Hence, the development of the catalyst-free methods for growing arrays of high quality, dense vertically aligned nanotubes is a pressing demand now. The metal-free nucleation and growth of carbon nanotubes is possible, yet with the use of other catalytic material, and with a low quality outcome. For example, the nucleation and growth on semiconductor nanoparticles in CVD process was recently reported [22,23,24]. In these works, the nanotubes were catalyzed and grown without metal catalyst, but those nanotubes are not vertically aligned but highly tangled, tousled, and the surface density is quite low. Therefore, obtaining high quality arrays of CNTs on a catalyst-free silicon substrate still remains elusive.
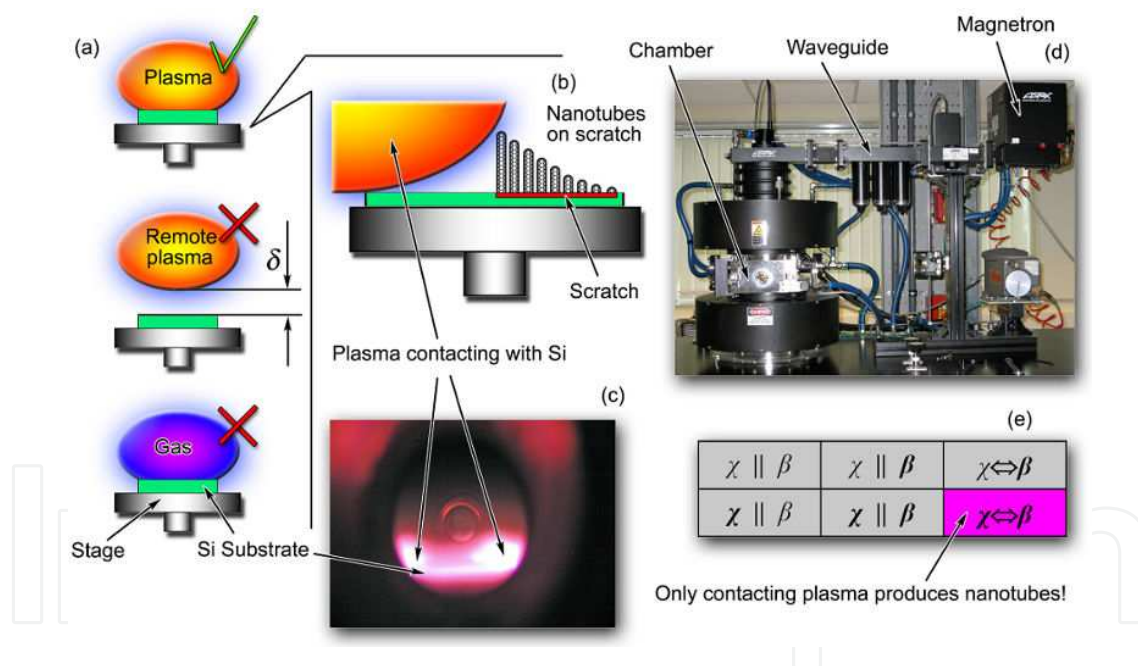

Figure 7. a) Three typical process configurations: localized plasma, remote plasma, gas environment; (b) nanotubes growth on Si substrate contacting with plasma: dense nanotubes as-grown on a doted spot; (c) photo of the plasma above substrate and (d) photo of the microwave reactor; (e) complete experiment matrix, which indicates the substrate condition (for scratched or non-scratched surface), and the process environment condition; remote gas/plasma and contacting gas/plasma. Among all possible 6 variants tested, only localized plasma process have produced nanotubes on substrate [25].
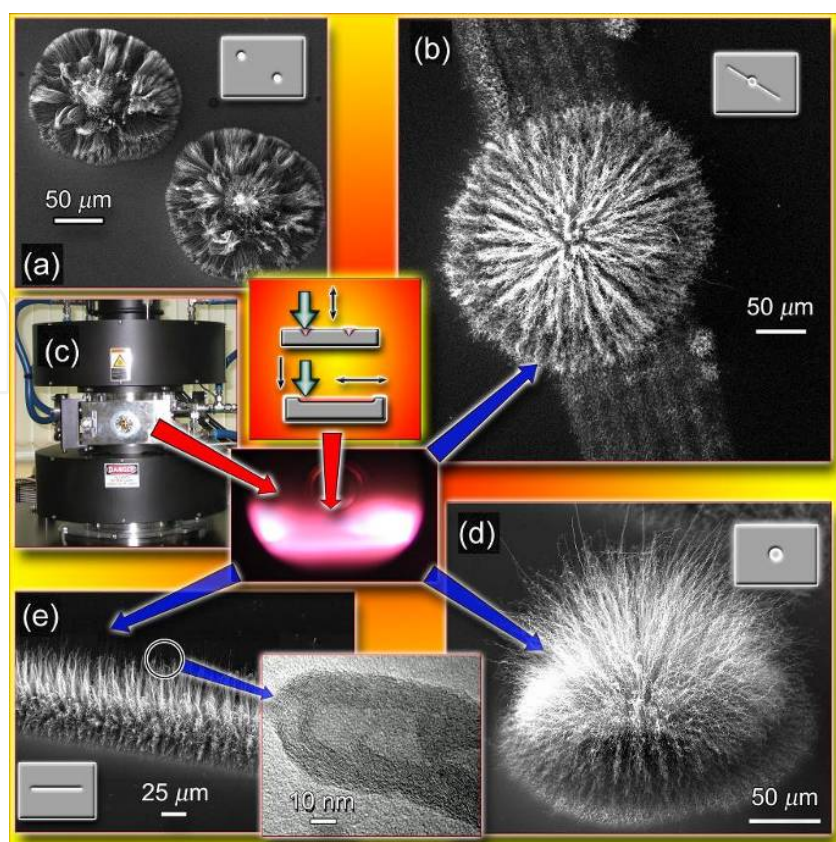
Figure 8. a,b) Top-view of CNTs on doted spots (SEM images); (c) microwave reactor; (d, e) tilted SEM image of CNT arrays showing a high number density of CNTs. Insets illustrate the process of making pattern and TEM image of the carbon nanotube [25].

Here we describe a novel plasma-based catalyst-free growth technique that is capable of producing very dense, strongly aligned arrays of extremely long (up to several hundred μm) CNTs on Si wafer surface in very fast process (with growth rate achieving 50 μm/sec), with experimentally proven possibility to arrange the nanotubes into complex arrays of various shapes such as separate nests and linear strands.

The six different experimental variations were used, with respect to the plasma/gas environments and plasma location relative to the substrate, as shown in Figure 7. We did not observe the nanotube nucleation in gas environment, on both smooth and patterned surfaces; we also did not observe the nucleation on both smooth and patterned surfaces with the remotely located plasma, and only the process conducted in plasma contacting the patterned surface resulted in the nucleation and growth of CNTs. The process starts by applying a special notch pattern (NP) on the prepared Si(100) wafers.

Then, the substrates with a specific NP (we used a linear NP consisting of parallel notches, and spot pattern of small pits) was treated in a chemical vapor deposition (CVD) reactor (Figure 8) where a microwave discharge was ignited in gas mixture of CH_4 and N_2, at pressure of 13 Torr and power density of 1.28 W/cm³, typically for 3 min. The substrates were heated up to ~800 °C only by the plasma. The plasma localization relative to the sub-

strate was varied to study in detail the plasma effect on CNT growth process (Figure 1e); namely, the process conducting with plasma contacting the wafer surface was effective for nucleation and growth of CNTs. More details on making the mechanical pattern are shown in Figure 8.

The scanning electron microscopy (SEM) investigations (Figure 9) show that a fast growth of a high-density, highly aligned CNTs are produced exactly replicating the pattern configuration (a complex pattern configuration which consists of a linear notch and spot applied directly on the notch have been achieved). The SEM images clearly show that the complex pattern of CNTs was perfectly replicated by nanotubes and the longest nanotubes reach ~140 μm in length. The growth sites are very densely occupied, and the rest wafer surface is absolutely free of nanotubes. Notably, these very dense arrays were formed in a very fast process, such unusual growth rates (up to ~48 μm/minute) were not reported previously in the absence of metal catalyst. Figure 9a shows the high-magnification SEM image of the nanotube array.
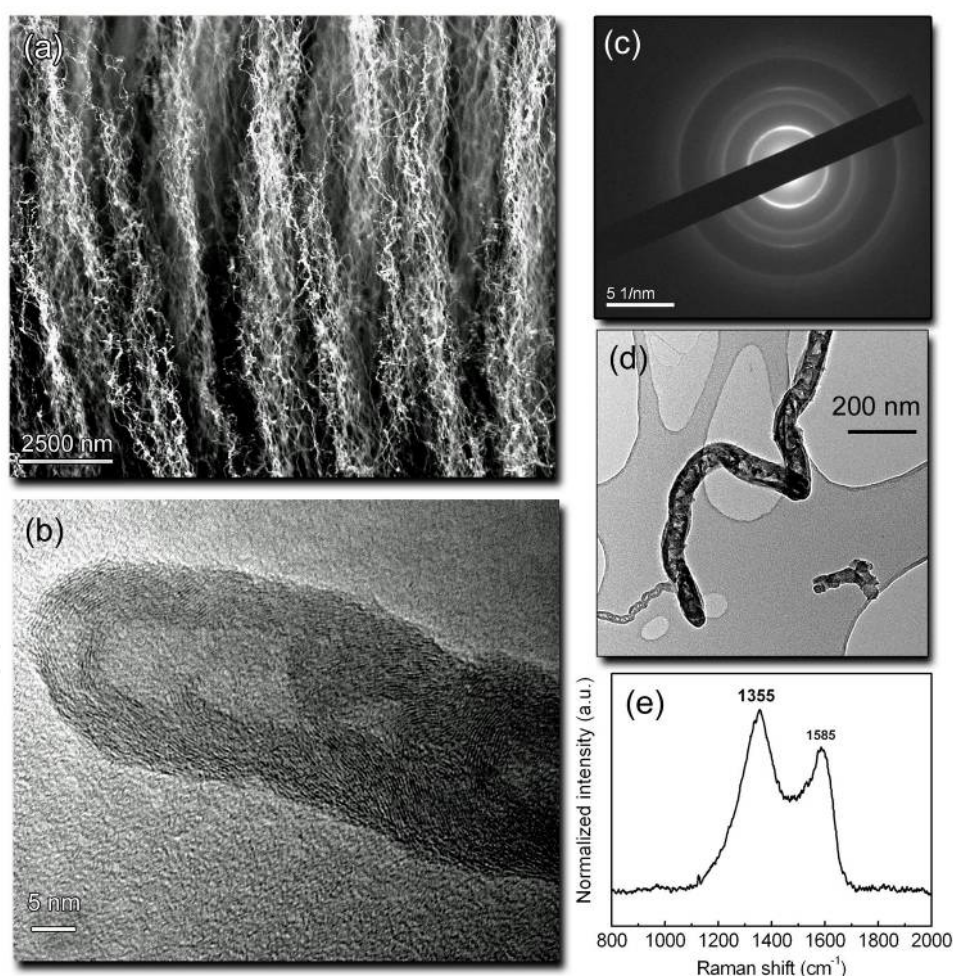
Figure 9. a) High-magnification SEM image of the vertically-oriented CNTs; (b) a high-resolution TEM image showing the planes in CNTs, with the inter-planer distance of ~0.34 nm; (c) the electron diffraction pattern of CNTs; (d) low-resolution TEM image showing the nanotube diameter of about 10 nm; (e) micro-Raman spectrum of the carbon nanotubes [25].

Further characterization of the nanotube structure was done with a high-resolution transmission electron microscopy (TEM) and Raman techniques (Figure 9). The TEM images (inset in Figure 8, Figures 9b and 9d) clearly show the absence of catalyst particle at the closed end tip of the CNTs, this reveals that the nanotubes were following in a "base-growth" mode [25]. As follows from TEM images, the diameters of the nanotubes are in the range of 10-80 nm, with up to 25 walls. Figure S13c shows the electron diffraction pattern of multi-wall nanotubes. Raman spectrum of as-grown nanotubes obtained at a room temperature (Figure 9e) shows a Raman broad-band peak at 1585 cm^{-1}, which is the characteristic of in-plane C-C stretching E2g mode of the hexagonal sheet. The appearance of a broad-band peak at 1355 cm^{-1} indicates the disordered graphitic nature of the nanotubes.

Thus, the nanotubes in our experiments were grown on the features mechanically written on the surface of Si wafer, and no nanotubes were formed on the intact silicon. To explain this, we propose a mechanism based on the key role of nano-elements on Si surface, so-called 'nano-hillocks'. These hillocks are formed on the surface when writing pattern, they establish a strong covalent bond to the Si surface at a temperature of ~800 °C during the process of CNT nucleation, and thus remain on Si surface, and hence at the bottom of nanotube during the whole growth process. Indeed, the solubility of carbon in Si is very low (10^{-3} %) [26] as compared to the conventional metallic catalyst such as Fe, Co, Ni etc., and thus the extremely high (up to 1 μm/s) growth rate observed in these experiments indicates that the nanotubes were grown via a surface diffusion, without involving very slow bulk-Si diffusion. Thus, a vapor-liquid-solid (VLS) mechanism was not involved, and the plasma played a key role in this process. We propose the following mechanism, so-called *reshaping-enhanced surface catalyzed* (RESC)growth. During the first stage, the tip region of a Si nano-hillock was heated up by plasma due to increased current density to the nano-sized tip (Figure 10).
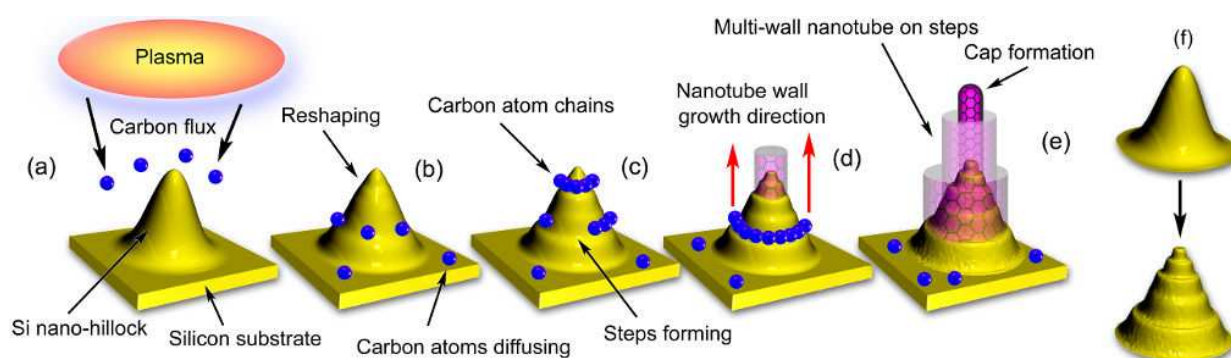

Figure 10. Scheme of the proposed mechanism of carbon nanotube nucleation and growth on silicon nano-hillocks in the plasma environment. (a) Si nano-hillock (with the shape 'as-produced' by mechanical patterning) is locally (mainly at the top) heated by the plasma; (b) heated Si nano-hillock starts reshaping – multiple step-like features are formed due to thermal re-arrangement and carbon saturation of the upper (overheated) Si layer; single carbon atoms incorporate into the steps; (c) reshaping continues, the steps become well-shaped, carbon atoms form chains (nanotube nuclei) along the multiple steps; (d) carbon chains close, nanotube start growing; (e) nanotube grow and close; (f) supposed reshaping of the silicon nano-hillock during plasma heating and nanotube nucleation [25].

Further, the heated silicon nano-hillock starts reshaping [27] by forming multiple step-like features due to thermal re-arrangement of silicon (to minimize the surface energy), and partially due to the possible carbon solution and saturation in the upper overheated Si layer. Then, carbon atoms incorporate into the steps and form closed chains. Simultaneously, the steps become well-shaped and thus carbon atoms assist the nanotube nucleation along the multiple steps. Later, multi-walled nanotubes start growing. Eventually, when the nanotube reaches 100-150 μm in length, the tip of carbon nanotube closes.

Thus, in this process the carbon catalization proceeds by the minimization of surface energy at the nano-hillock steps [28], since the adatom adsorbed in the step can be considered as 'partially dissolved'. As a result, this process leads to the formation of very dense array of very long multiwall nanotubes on the mechanically patterned areas. Thus, the proposed growth mechanism explains all the observed features; it is noteworthy that just the effect of plasma on the patterned surface explains several important characteristics due to plasma-related heating and high rate of material delivery. As a result, the catalyst-free, very dense arrays of long (up to 150 μm) vertically oriented multiwall carbon nanotubes were grown on the mechanically patterned silicon wafers in a low-temperature microwave discharge. These experiments have demonstrated an extremely high (up to 48 μm/min) growth rate.

4. Three-dimensional CNT arrays by post-processing with liquids

The above-described method can be used to produce 'planar', drawing-like arrays of the verti‐ cally-aligned carbon nanotubes on silicon surfaces. When a need in a complex three-dimen‐ sional array arises, post-processing of the uniform array (array-precursor) can be used. Among others, the post-treatment with a liquid is the most cheap and convenient [29-38]. Nevertheless, this technique still lacks controllability. In this section we show several possible ways of en‐ hancing controllability of the fabrication of three-dimensional structures of the vertically-aligned carbon nanotube arrays. Specifically, we show that the array structure can be a key factor of the resultant structure fabricated by immersing the CNT array into liquid.

Figure 11a is an SEM image of the cross-section of the array of vertically-aligned CNTs grown using the CVD technique. This array exhibits super hydrophobic properties and thus, it cannot be wetted by water. After immersing into water, only weakly-collapsed irregular structure was produced (Figure 11b). In contrast, this array does not show super-hydrofobicity to acetone, and thus, highly-regular completely collapsed pattern was produced by immersing this array into acetone (Figures 11c, 11d). As one can see in this figure, this pattern exhibits very high surface area of the 'sponge', produced by carbon nanotubes (and hence, the walls of this sponge can be highly-conductive or semi-conductive). Such structures could be very useful for the fabrication of gas and bio-sensors, gas storage devices, as well as energy-transforming applications requiring very high levels of the light absorbance.

It is apparent that the control over the resultant structure of such patterns is a key issue for the above applications. Using different growth conditions, we have grown a similar CNT array with denser structure (see Figure 12a), which does not exhibit super-hydrophobic properties.
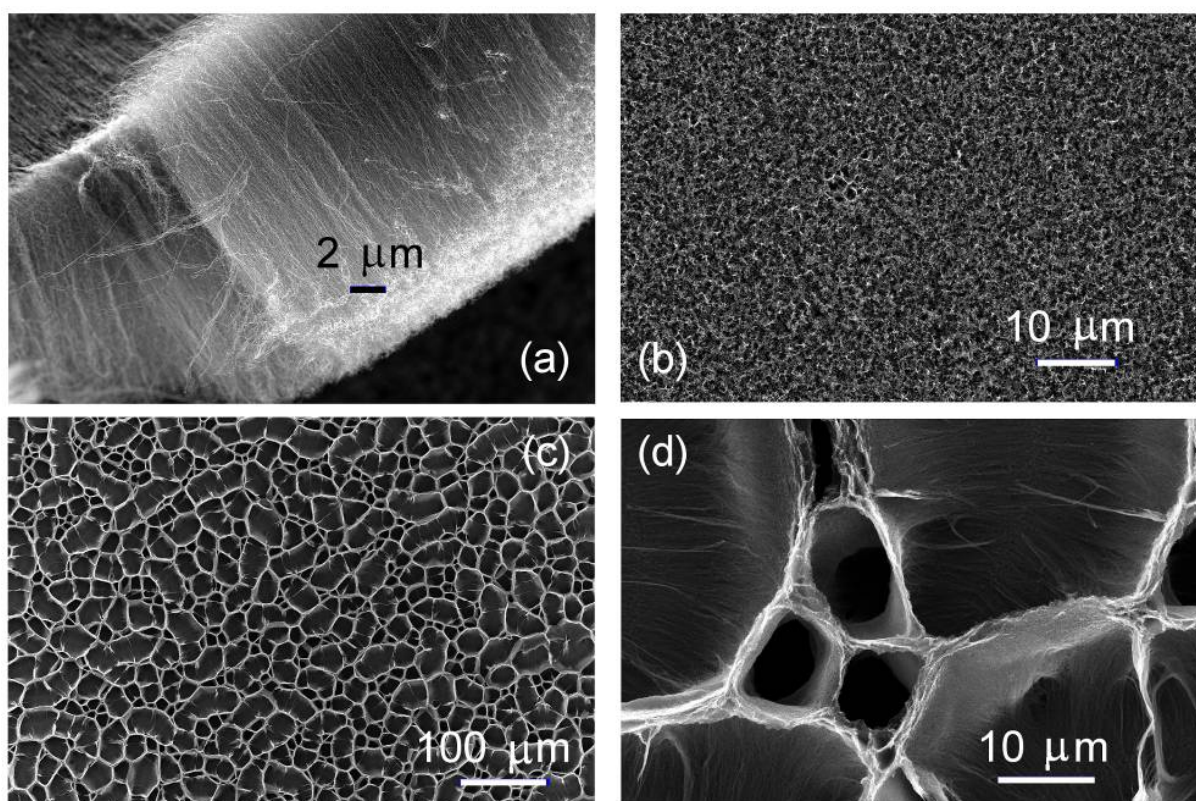
Figure 11. Treatment of super-hydrophobic sample with water and acetone. (a) Cross-section of the arrays of vertically-aligned nanotubes. (b) Irregular structure was produced after treating with water. (c, d) Regular structure (completely collapsed pattern) was produced by acetone, low and high magnifications.

Post-treatment of this array with ethanol and acetone has produced the sponge-like structure consisting of separated fine-porous island (Figures 12b, c, d). This structure is significantly different of that fabricated using super-hydrophobic sample (Figure 11). Moreover, variation of the dosage of liquid (we used 5 and 10 droplets of acetone, applied in sequence after complete drying of the preciously-applied drop) can be used to slightly change the structure. A comparison of the structures produced by 5 and 10 drops (Figures 12c and d) reveals a slight change in the pore sizes.

The use of water to treat this weakly hydrophobic CNT array produces slightly different pattern (Figure 13) consisting of smaller islands, which still demonstrate the sponge-like structure, i.e., each island is not a solid, intact array of the vertically-aligned carbon nanotubes but also consists of collapsed CNTs forming fine pores. One can expect that the fine-sponged structures produced using weakly hydrophobic CNT arrays can be very promised for the gas storage applications, whereas the highly-collapsed patterns may be more promising for sensing and other applications requiring control of the electrical resistivity of the surface. Thus, different internal structure of the vertically-aligned CNT array, together with the type of liquid and dosage, can be control parameters for the production of CNT patterns with a high level of the controllability.
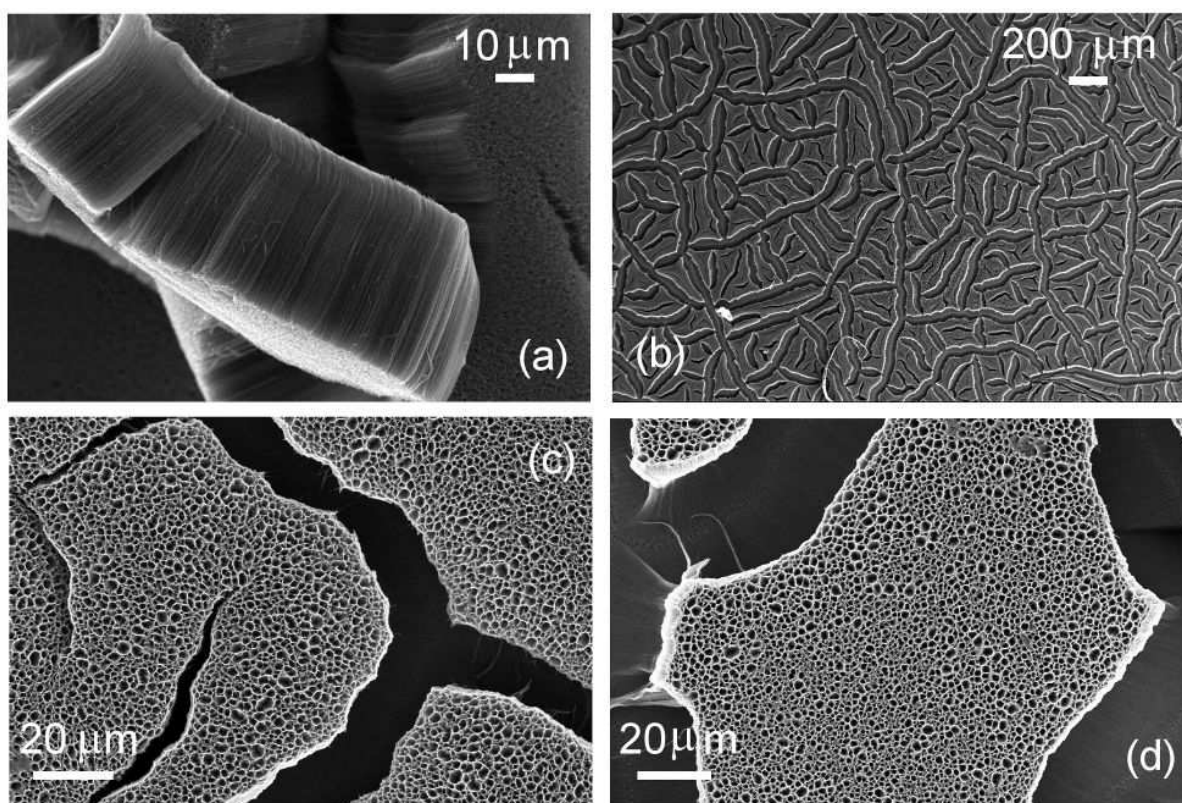
Figure 12. Treatment of weakly hydrophobic CNT array (a) with ethanol (b) and acetone, application of 5 drops (c) and 10 drops (d). Acetone produces a patterned sponge-like structure consisting of fine-porous island.
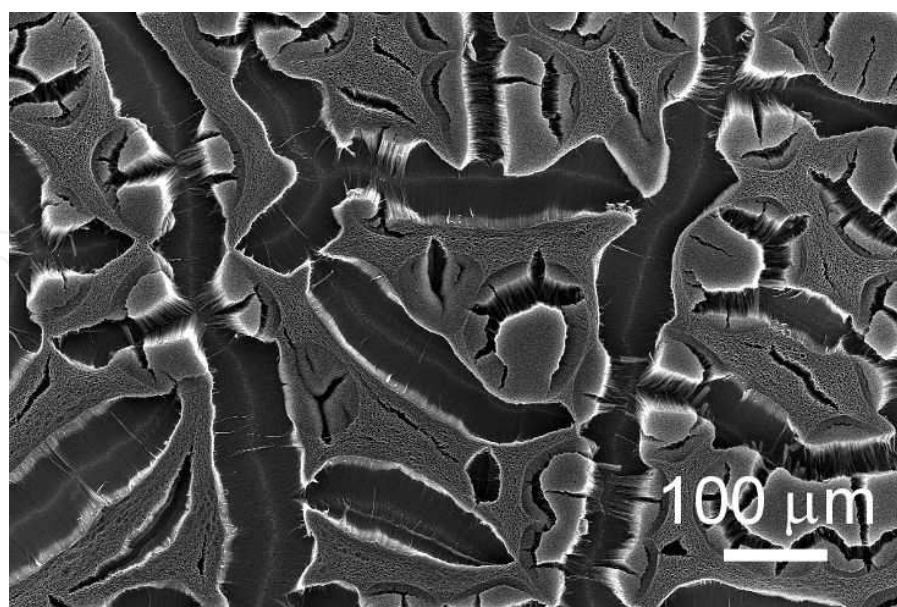

Figure 13. Treatment of weakly hydrophobic sample with water. Smaller islands demonstrate the sponge-like structure.

5. Perspective approaches for the control of array morphology

Dense arrays of highly ordered surface-bound vertically aligned nanotubes on silicon and metal oxides have a great potential for the fabrication of various advanced nano- and micro-devices such as fuel cells, sensors, and field emission element [39,40,41,42] One possible way to integrate the carbon nanotube array in the silicon platform is the use of anodized aluminum oxide (AAO) membranes to grow the pre-structured CNT patterns, bonded to the template surface. Indeed, the use of AAO membranes as growth templates was successful for the fabrication of, i.e., electron emitters [43]. Synthesis of carbon nanotubes on AAO templates allows precise and reproducible control of the dimensions of nanotubes [44, 45]. In this section we will review in short the AAO template characteristics important for growing the carbon nanotube arrays, and discuss the most important control parameters.

An AAO template can be prepared by the anodic oxidation of aluminum in various acid solutions. The thickness, pore size and interpore distance can be easily controlled by varying conditions of anodization such as composition of electrolyte, process temperature, applied voltage, process time and pore widening time [46,47]. Figure 14 shows SEM images of the free standing AAO templates fabricated by the two-step anodization.
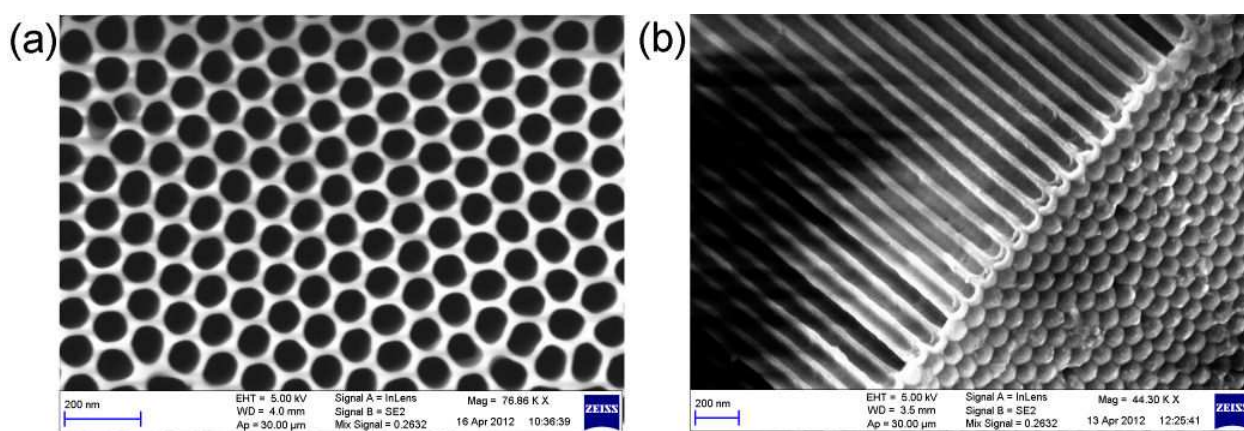

Figure 14. A Free-standing AAO fabricated using a two-step anodization. (a) Top view and (b) side view.

However, the free-standing AAO templates and membranes fabricated on aluminum foil are not be suitable for growing carbon nanotube arrays due to the thermal instability. Under thermal treatment, which is inevitable in the nanotube fabrication process, the AAO templates fabricated on aluminum foil easily crack due to the difference in thermal expansion coefficient of the alumina oxide and underlying aluminum. Moreover, the growth temperature cannot exceed the aluminum melting point e. In addition, a free-standing AAO template easily cracks due to its ceramic nature. Therefore, the conventional approach based on the use of the aluminum foil is not suitable for the CNT growth and fabrication of the carbon nanotube-based electronic devices.

To avoid this problem, it is necessary to fabricate AAO templates on other functional substrates. The alternative materials include silicon, quartz and ITO glass, on which the highly

ordered structure of very thin AAO templates can be fabricated. For example, AAO templates fabricated on silicon wafers have already been used to fabricate highly ordered carbon nanotubes [48]. The AAO templates fabricated on non-aluminum substrates can be compatible with much higher processing temperatures, well above the 700 °C. Silicon substrates may be also useful for protecting AAO from distortion during the CNT growth.

However, quartz is more advantageous substrate for AAO membranes to be used as templates for the CNT synthesis. Quartz has a very high melting point, allowing for much higher temperatures, and can protect the AAO templates from cracking during the thermal treatment. Another advantage of quartz is transparency enabling the use of AAO templates as photonic crystals, and thus significantly broadening the application of fabricated AAO templates in other optics related applications.
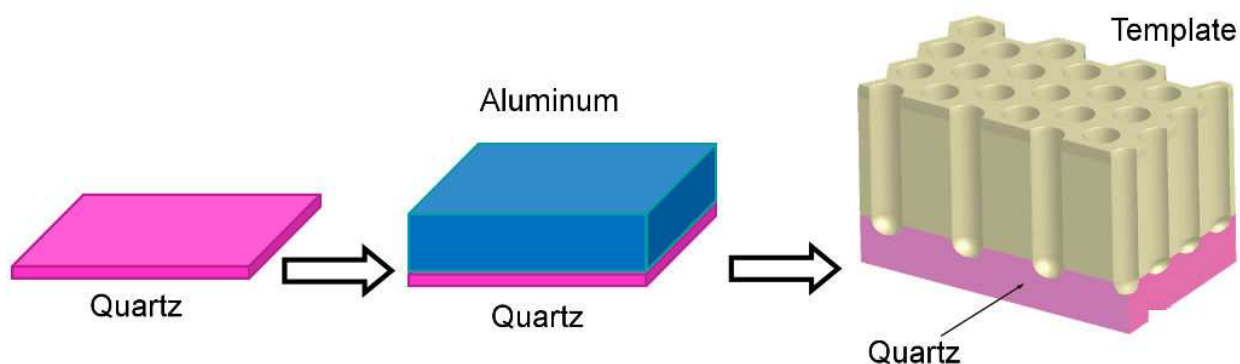

Figure 15. Schematic of the fabrication of AAO on quartz. High purity aluminum is deposited onto cleaned quartz, and the template is fabricated by anodization.
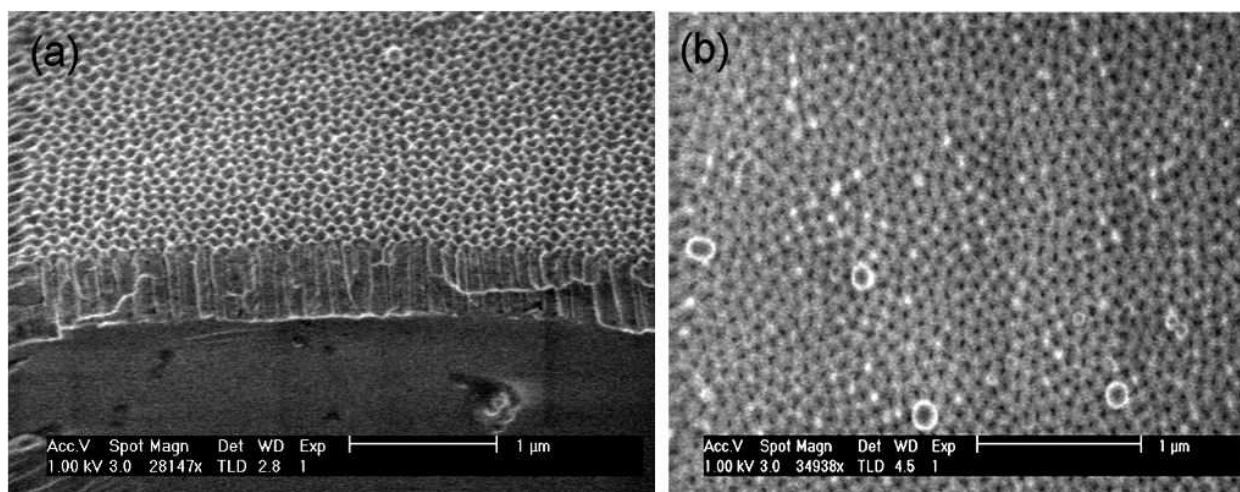

Figure 16. SEM images of the quartz-based AAO template suitable for the fabrication of carbon nanotube arrays. (a) Side view and (b) top view.

The high quality AAO templates were fabricated directly on quartz, using a two-step anodization without using any inter-layers between the deposited aluminum and quartz substrate. Figure 15 illustrates the schematic of this process. Prior to the fabrication of AAO template, quartz samples are cleaned in boiling solution of 30% w.t. of H_2SO_4 and 70% W.t. of H_2O_2. After that, the samples were etched in HF solution (0.1 w.t.% for 30 seconds), placed into an e-beam evaporator and coated with high purity (99.999%) aluminum to a thickness of 1.0 μm at a deposition rate of ≈1.5 nm×s^{-1}. The deposited Al film was then anodized to produce porous alumina templates in an electrolytic cell using a two-step anodization process. As a result, high quality AAO templates on quartz were fabricated. Figure 16 shows the SEM image of the AAO templates.

Above results demonstrate that AAO template technology not only can be used in a piece of aluminum foil, but also can be combined with silicon and other functional substrate technology. AAO template on functional substrate were used in the fabrication of CNT arrays can be realize the field emitters or possible become optical devices when CNT in quartz-AAO. Moreover, since the crystallinity of CNTs increase with the synthesis temperature, the emission current density increases with the synthesis temperature of CNTs. This again demonstrated that only AAO on functional substrate can realize high quality of CNTs array fabrication.

Author details

I. Levchenko[1,2], Z.-J. Han[1,2], S. Kumar[1,2], S. Yick[1,2], J. Fang[1,3] and K. Ostrikov[1,2]

1 Plasma Nanoscience Centre Australia (PNCA), CSIRO Materials Science and Engineering, Lindfield, Australia

2 Plasma Nanoscience, School of Physics, The University of Sydney, Sydney, Australia

3 School of Physics, The University of Melbourne, Parkville, VIC, Australia

References

[1] C. A. Crouse, B. Maruyama, R. Colorado Jr., T. Back, A. R. Barron. Growth, new growth, and amplification of carbon nanotubes as a function of catalyst composition. J. Am. Chem. Soc. 2008;130(25), 7946–7954.

[2] Z.-J. Han, I. Levchenko, S. Yick, K. Ostrikov. 3-Orders-of-magnitude density control of single-walled carbon nanotube networks by maximizing catalyst activation and dosing carbon supply. Nanoscale 2011;3, 4848-4853.

[3] Z.-J. Han, S. Yick, I. Levchenko, E. Tam, M. M. A. Yajadda, S. Kumar, P. J. Martin, S. Furman, K. Ostrikov. Controlled synthesis of a large fraction of metallic single-wal-

led carbon nanotube and semiconducting carbon nanowire networks. Nanoscale 2011;3, 3214-3220.

[4] Z. J. Han, B. K. Tay, M. Shakerzadeh, K. Ostrikov. Superhydrophobic amorphous carbon/carbon nanotube nanocomposites. Appl. Phys. Lett. 2009;94, 223106.

[5] I. Levchenko and K. Ostrikov, M. Keidar, S. Xu. Deterministic nanoassembly: Neutral or plasma route? Appl. Phys. Lett. 2006;89, 033109.

[6] M Meyyappan. A review of plasma enhanced chemical vapour deposition of carbon nanotubes. J. Phys. D: Appl. Phys. 2009;42, 213001.

[7] W. Zhou, L. Ding, S. Yang, J. Liu. Synthesis of high-density, large-diameter, and aligned single-walled carbon nanotubes by multiple-cycle growth methods. ACS Nano 2011;5, 3849–3857.

[8] K. Hata, D. N. Futaba, K. Mizuno, T. Namai, M. Yumura, S. Iijima. Water-assisted highly efficient synthesis of impurity-free single-walled carbon nanotubes. Science 12004;306, 1362-1364.

[9] G. Zhang, D. Mann, L. Zhang, A. Javey, Y. Li, E. Yenilmez, Q. Wang, J. P. McVittie, Y. Nishi, J. Gibbons, H. Dai. Ultra-high-yield growth of vertical single-walled carbon nanotubes: Hidden roles of hydrogen and oxygen. PNAS 2005;102, 16141-16145.

[10] D. Sun, M. Y. Timmermans, Y. Tian, A. G. Nasibulin, E. I. Kauppinen, S. Kishimoto, T. Mizutani, Y. Ohno. Flexible high-performance carbon nanotube integrated circuits. Nature Nanotech. 2011;6, 156–161

[11] J. Wu, K. S. Paudel, C. Strasinger, D. Hammell, A. L. Stinchcomb, and B. J. Hinds, Programmable transdermal drug delivery of nicotine using carbon nanotube membranes. Proc. Natl. Acad. Sci. USA 2010;107, 11698.

[12] Z. J. Han, K. Ostrikov, C. M. Tan, B. K. Tay, S. A. F. Peel. Effect of hydrophilicity of carbon nanotube arrays on the release rate and activity of recombinant human bone morphogenetic protein-2. Nanotechnology 2011;22, 295712.

[13] S. Kumar, I. Levchenko, Q. J. Cheng, J. Shieh, K. Ostrikov. Plasma enables edge-to-center-oriented graphene nanoarrays on Si nanograss. Appl. Phys. Lett. 2012;100, 053115.

[14] Z. J. Han, K. Ostrikov. Uniform, dense arrays of vertically aligned, large-diameter single-walled carbon nanotubes. J. Am. Chem. Soc. 2012;134, 6018–6024.

[15] M. P. Garrett, I. N. Ivanov, R. A. Gerhardt2,3, Alex A. Puretzky2, and David B. Geohegan. Separation of junction and bundle resistance in single wall carbon nanotube percolation networks by impedance spectroscopy Appl. Phys. Lett. 97, 163105 (2010); http://dx.doi.org/10.1063/1.3490650 (3 pages)

[16] Q. Cao, H. Kim, N. Pimparkar, J. P. Kulkarni, C. Wang, M. Shim, K. Roy, M. A. Alam, J. A. Rogers. Medium-scale carbon nanotube thin-film integrated circuits on flexible plastic substrates. Nature 2008;454, 495-500.

[17] M. A. Topinka, M. W. Rowell, D. Goldhaber-Gordon, M. D. McGehee, D. S. Hecht, G. Gruner. Charge transport in interpenetrating networks of semiconducting and metallic carbon nanotubes. Nano Letters 2009;9, 1866–1871.

[18] K. Ostrikov. Reactive plasmas as a versatile nanofabrication tool. Rev. Mod. Phys. 2005;77, 489–511.

[19] Z. J. Han, H. Mehdipour, X. Li, J. Shen, L. Randeniya, H. Y. Yang, K. Ostrikov. SWCNT networks on nanoporous silica catalyst support: morphological and connectivity control for nanoelectronic, gas-sensing, and biosensing devices. ACS Nano 2012;6, 5809–5819.

[20] T. W. Ebbesen, P. M. Ajayan, H. Hiura, K. Tanigaki. Purification of nanotubes. Nature 1994;367 519-page.

[21] X. M. H. Huang, R. Caldwell, L. Huang, S. C. Jun, M. Huang, M. Y. Sfeir, S. P. O'Brien, J. Hone. Controlled Placement of Individual Carbon Nanotubes Nano Letters 2005;5 1515.

[22] D. Takagi, H. Hibino, S. Suzuki, Y. Kobayshi, and Y. Homma. Carbon Nanotube Growth from Semiconductor Nanoparticles. Nano Letters 2007;7(8) 2272-page.

[23] B. Liu, W. Ren, L. Gao, S. Li, S. Pei, C. Liu, C. Jiang and H. M. Cheng. Metal-Catalyst-Free Growth of Single-Walled Carbon Nanotubes. J. Am. Chem. Soc. 2009;131 2082.

[24] S. Huang, Q. Cai, J. Chen, Y. Qian, and L. Zhang. Metal-Catalyst-Free Growth of Single-Walled Carbon Nanotubes on Substrates. J. Am. Chem. Soc. 2009;131, 2094-page.

[25] S. Kumar, I. Levchenko, K. Ostrikov and J. McLaughlin. Plasma-enabled, catalyst-free growth of carbon nanotubes on mechanically-written Si features with arbitrary shape. Carbon 2012, 50, 321.

[26] P. Laveant, P. Werner, G. Gerth, and U.Gosele. Incorporation, diffusion and agglomeration of carbon in silicon. Solid State Phenomeona 2002;82-84, 189.

[27] S. Helveg, C. Lopez-Cartes, J. Sehested, P. L. Hansen, B. S. Clausen, J. R. Rostrup-Nielsen, F. Abild-Pedersen, J. K. Norskov. Atomic-scale imaging of carbon nanofibre growth. Nature 2004;427, 426.

[28] J. Pezoldt, Y. V. Trushin, V. S. Kharlamov, A. A. Schmidt, V. Cimalla, O. Ambacher. Nuclear Instr. Meth. in Phys. Res. B 2006;253, 241.

[29] E.M. Kotsalisa, E. Demosthenousb, J.H. Walthera, c, S.C. Kassinosb, P. Koumoutsakos. Wetting of doped carbon nanotubes by water droplets. Chem. Phys. Lett. 2005;412, 250–254.

[30] M. A. Correa-Duarte, N. Wagner, J. Rojas-Chapana, C. Morsczeck, M. Thie, M. Giersig. Fabrication and Biocompatibility of Carbon Nanotube-Based 3D Networks as Scaffolds for Cell Seeding and Growth. Nano Lett. 2004;4 2233-2236.

[31] B. Q. Wei, R. Vajtai, Y. Jung, J. Ward, R. Zhang, G. Ramanath, P. M. Ajayan. Organized assembly of carbon nanotubes. Nature 2002; 416, 495-496.

[32] C. L. Pint, Y.-Q. Xu, M. Pasquali, R. H. Hauge. Formation of Highly Dense Aligned Ribbons and Transparent Films of Single-Walled Carbon Nanotubes Directly from Carpets. ACS Nano 2008;2, 1871–1878.

[33] B. Pokroy, S. H. Kang, L. Mahadevan, J. Aizenberg. Self-Organization of a Mesoscale Bristle into Ordered, Hierarchical Helical Assemblies. Science 2009; 323, 237-240.

[34] D. N. Futaba, K. Hata, T. Yamada, T. Hiraoka, Y. Hayamizu, Y. Kakudate, O. Tanaike, H. Hatori, M. Yumura, S. Iijima. Shape-engineerable and highly densely packed single-walled carbon nanotubes and their application as super-capacitor electrodes. Nature Materials 2006;5, 987-994.

[35] S. Li, H. Li, X. Wang, Y. Song, Y. Liu, L. Jiang, D. Zhu. Super-hydrophobicity of large-area honeycomb-like aligned carbon nanotubes. J. Phys. Chem. B 2002;106, 9274-9276.

[36] W. Wang, M. Tian, A. Abdulagatov, S. M. George, Y.-C. Lee, R. Yang. Three-dimensional Ni/TiO2 nanowire network for high areal capacity lithium ion microbattery applications. Nano Lett. 2012;12, 655–660.

[37] H. Liu, J. Zhaia, L. Jiang. Wetting and anti-wetting on aligned carbon nanotube films. Soft Matter. 2006;2, 811–821.

[38] C. T. Wirth, S. Hofmann, J. Robertson. Surface properties of vertically aligned carbon nanotube arrays. Diam. Relat. Mater. 2008;17, 1518–1524.

[39] Z. Wang, L. Ci, L. Chen, S. Nayak, P. M. Ajayan and N. Koratkar. Polarity-Dependent Electrochemically Controlled Transport of Water through Carbon Nanotube Membranes. Nano Letters 2007;7, 697.

[40] K. Gong, F. Du, Z. Xia, M. Durstock and L. Dai. Nitrogen-doped carbon nanotube arrays with high electrocatalytic activity for oxygen reduction. Science 2009;323, 760.

[41] I. Levchenko, S.Kumar, M. M. A. Yajadda, Z. J. Han, S. Furman, K. Ostrikov. Self-organization in arrays of surface-grown nanoparticles: characterization, control, driving forces. J. Phys. D: Appl. Phys. 2011;44, 174020.

[42] M. E. Itkis, A. Yu and R. C. Haddon. Single-Walled Carbon Nanotube Thin Film Emitter–Detector Integrated Optoelectronic Device. Nano Letters 2008;8, 2224.

[43] S.-K. Hwang, J. Lee, S.-H. Jeong, P.-S. Leen, K.-H. Lee. Fabrication of carbon nanotube emitters in an anodic aluminum oxide nanotemplate on a Si wafer by multi-step anodization. Nanotechnology 2005;16, 850–858.

[44] K. Liu, M. Burghard and S. Roth. Conductance spikes in single-walled carbon nanotube field-effect transistor. Appl. Phys. Lett. 1999;75, 2494.

[45] J. S. Suh, J. S. Lee. Highly ordered two-dimensional carbon nanotube arrays. Appl. Phys. Lett. 1999;75 2047.

[46] J. Fang, P. Spizzirri, A. Cimmino, S. Rubanov, and S. Prawer, Nanotechnology, 20, 065706 (2009). Extremely high aspect ratio alumina transmission nanomasks: their fabrication and characterization using electron microscopy.

[47] A. P. Li, F. Müller, A. Birner, K. Nielsch, U. Gösele. Hexagonal pore arrays with a 50–420 nm interpore distance formed by self-organization in anodic alumina. J. Appl. Phys. 1998;84, 6023.

[48] S. Chu, K.Wada, S. Inoue, S. Todoroki. Synthesis and characterization of titania nanostructures on glass by Al anodization and sol-gel process. Chem. Mat. 2002;14(1), 266.